

VII International Conference on Computational Methods for Coupled Problems in Science and Engineering  
COUPLED PROBLEMS 2017  
M. Papadrakakis, E. Oñate and B. Schrefler (Eds)

## NOVEL KINETIC CONSISTENT ALGORITHM FOR THE MODELING OF INCOMPRESSIBLE CONDUCTING FLOWS

B. CHETVERUSHKIN\*, N. D'ASCENZO\*\*† , A.SAVELIEV\*\*†  
AND V. SAVELIEV\*\*†

\* Keldysh Institute of Applied Mathematics  
Russian Academy of Science (KIAM RAS)  
4 Miusskaya sq, 125047 Moscow, Russia  
e-mail: chetver@imamod.ru, web page: <http://www.kiam.ru>

†Deutsches Elektronen Synchrotron (DESY)  
85 Notkestrasse, 22607 Hamburg, Germany  
e-mail: ndasc@mail.desy.de - Web page: <http://www.desy.de>

††Hamburg University  
85 Notkestrasse, 22607 Hamburg, Germany  
e-mail: Andrey.Saveliev@desy.de - Web page: <http://www.desy.de>

\*\* Immanuel Kant Baltic Federal University  
14 Alexandr Nevsky str., 236016, Kaliningrad, Russia  
e-mail: saveliev@mail.desy.de - Web page <http://www.kantiana.ru>

**Key words:** MGD pump, numerical methods, kinetic consistent algorithms

**Abstract.** In this study we aim at demonstrating that kinetic consistent magneto gas dynamic algorithms are a valid for the computation of the dynamics of incompressible conductive flows. We obtain numerical solutions for the test problems, namely the laminar flow inside a wall-driven cavity and a magnetic driven pump. We show that kinetic consistent algorithms have a high stability in the solution of convection-dominated flows, due to a correct physical modeling of the fluid viscosity and to the possibility of tuning appropriate regularization terms on the basis of the physical properties of the fluid. We show that the kinetic consistent approach offers a stable basis for a correct physical description of the shear viscosity, thermal conduction and electric resistivity effects in incompressible magneto hydrodynamics flows.

### 1 INTRODUCTION

Recently many important critical technical applications are based on the magnetohydrodynamic principles. The magnetohydrodynamic pumping (MHP) of electrically con-

ductive fluid is of growing interest for many industrial applications requiring precise flow control, especially in the critical conditions, enabling to break the flow or reverse flow direction without any moving parts or mechanical devices. Today, different MHD pump systems are widely used in many metal melting environments such as, among others, extrusion billet casting, metal refinery for transporting molten metals, liquid metal circulation for alloys production. These pumps have many advantages over the mechanical pumps including precise flow control, reduced energy consumption and less dross formation.

In the recent publications of the authors [1, 2], using a complex statistical distribution function and kinetic consistent scheme, it was investigated the effective numerical algorithm for the parallel high performance computing systems for the solution of the magneto gas dynamic problems. In [2] the results were presented of the mathematical modeling of the accretion processes of interstellar matter on the compact massive astrophysical object. We investigated the three dimensional system of differential equations including the three dimensional equation of the magnetic induction with the magnetic viscosity.

The goal of the present study is the extension of the proposed kinetic consistent magneto gas dynamic algorithms, efficient with numerical computations on the detailed space mesh, more than  $10^9$  cells, for the mathematical modeling of the conducting incompressible liquid flows.

In common approaches the algorithms of mathematical modeling of incompressible liquids are dramatically different from viscous heat conductive magneto gas dynamics algorithms. The present study, based on the "equivalence" of the gases with Mach numbers less than 0.1, investigated the possibility of using the method of magneto gas dynamics with minimal changes for the mathematical modeling of the incompressible conductive liquid flow.

## 2 Mathematical Model

The sound speed in liquids is significantly higher than in gases. Taking into account that in technological systems the characteristic velocities is of the order of few meters per second the condition

$$U \leq 0.1M \tag{1}$$

is fully satisfied.

The state equation (artificial) can be formulated as

$$P = P_0 + \beta(\rho - \rho_0) \tag{2}$$

where the parameter  $\beta$  should define the condition of strong changes of the pressure with smallest changes in density.

In this conditions the kinetic consistent system of equations is :

$$\frac{\partial \rho}{\partial t} + \frac{\tau}{2} \frac{\partial^2 \rho}{\partial t^2} + \frac{\partial}{\partial x_i} \rho u_i = \frac{\partial}{\partial x_i} \left( \frac{\tau}{2} \frac{\partial}{\partial x_k} \Pi_{ik} \right) \quad (3)$$

$$\frac{\partial \rho u_i}{\partial t} + \frac{\tau}{2} \frac{\partial^2 \rho u_i}{\partial t^2} + \frac{\partial}{\partial x_k} \Pi_{ik} = \frac{\partial}{\partial x_k} \Pi_{ik}^D + \frac{\partial}{\partial x_k} \left[ \left( \frac{\tau}{2} \frac{\partial}{\partial x_k} \Pi_{ik} \right) u_k \right] \quad (4)$$

$$\begin{aligned} \frac{\partial E}{\partial t} + \frac{\tau}{2} \frac{\partial^2 E}{\partial t^2} + \frac{\partial F_i}{\partial x_i} &= \frac{\partial Q_i}{\partial x_i} + \frac{\partial}{\partial x_i} \Pi_{ik}^D u_k - B_k \Pi_{ik}^{DB} \\ &+ \frac{\partial}{\partial x_i} \left[ \frac{1}{\rho} \left( E + p + \frac{B^2}{8\pi} \right) \left( \frac{\tau}{2} \frac{\partial}{\partial x_k} \Pi_{ik} \right) \right] \end{aligned} \quad (5)$$

$$\frac{\partial B_i}{\partial t} + \frac{\tau_M}{2} \frac{\partial^2 B_i}{\partial t^2} + \frac{\partial}{\partial x_k} M_{ik}^B = \frac{\partial}{\partial x_k} \Pi_{ik}^{DB} \quad (6)$$

where the fluxes are:

$$\Pi_{ik} = \left( p + \frac{B^2}{8\pi} \right) \delta_{ik} + \rho u_i u_k - \frac{B_i B_k}{4\pi} \quad (7)$$

$$F_i = \left[ \left( E + p + \frac{B^2}{8\pi} \right) u_i - \frac{B_i u_k B_k}{4\pi} \right] \quad (8)$$

$$M_{ik}^B = u_k B_i - u_i B_k \quad (9)$$

$$\Pi_{ik}^D = \frac{\tau}{2} \left[ p \frac{\partial u_i}{\partial x_k} + p \frac{\partial u_k}{\partial x_i} - \frac{2}{3} p \frac{\partial u_m}{\partial x_m} \delta_{ik} \right] + O(Ma^2) \quad (10)$$

$$Q_i^D = \frac{\tau}{2} \left[ \frac{5}{2} p \frac{\partial p}{\partial x_i} \right] + O(Ma^2) \quad (11)$$

$$\Pi_{ik}^{DB} = \frac{\tau_M}{2} \left[ \frac{1}{\rho} \left( p + \frac{B^2}{8\pi} \right) \left( \frac{\partial B_i}{\partial x_k} - \frac{\partial B_k}{\partial x_i} \right) \right] + O(Ma^2) \quad (12)$$

On the left-hand side of the system of Eqs. 3-6 we retrieve the ideal magneto gas dynamics fluxes, which are extensively expressed in the first three terms of Eq. 12. The respective fluxes are the momentum, heat and magnetic field flux of the ideal magneto gas dynamics.

On the right-hand side of the system of Eqs. 3-6 we obtain additional dissipative terms. We have shown in [2] that the leading dissipative terms correspond to the Navier-Stokes and the physical resistivity, the additional dissipative terms being a smaller order computational stabiliser. The respective fluxes are extensively expressed in the last three terms of Eq. 12. They are the Navier-Stokes momentum and thermal flux and the additional magnetic flux due to the finite resistivity. We note here that, in comparison with the dissipative fluxes proposed in [2], the correction of  $O(Ma^2)$  are neglected, as we deal with low Mach number  $Ma$  problems in this study.

### 3 NUMERICAL EXAMPLES

#### 3.1 Lid driven cavity

This test is presented in [4, 5]. Here we use the same normalized units thereby defined for a better comparison of the results. A cavity filled in with fluid is defined on the two-dimensional domain  $[0, 1] \times [0, 1]$ . At the initial time the fluid is at rest, its density is constant and equal to  $\rho_0 = 1$ , its pressure is constant and equal to  $p_0 = \gamma^{-1}Ma^{-2}$ . The Mach number  $Ma = 0.15$  and the adiabatic constant  $\gamma = 1.4$  are used. The magnetic field is absent. The simulation is performed with different numbers of the Reynolds number  $Re = 400, 1000, 3400$ . The chosen set of parameters defines the fluid viscosity and the thermal conductivity:

$$\mu = \frac{Ma \cdot c}{Re} \quad k = \frac{\mu}{\gamma - 1} \quad (13)$$

where  $c$  is the thermal velocity of the fluid  $c = \sqrt{\gamma p / \rho}$ . The value of  $\tau$  in the kinetic algorithm is:

$$\tau = \frac{\mu}{p} + \alpha \frac{h}{c} \quad (14)$$

where  $h$  is the mesh size. The computational domain is divided into a mesh of  $128 \times 128$  cells in order to provide a direct comparison with [4]. The boundary conditions are open for all variables, except for the velocity, which is set to 0 on the  $x = 0, x = 1, z = 0$  borders and to 1 on the  $z = 1$  border.

Although this numerical example does not include the magnetic field, it provides a solid and well-established test for the gas dynamic components of the kinetic algorithm. The solution presents in fact a regular turbulent structure, with vortexes at a position and size confirmed by a large number of theoretical and experimental studies. In comparison with the traditional approaches [4], the set of kinetic consistent equations used in this study includes the density continuity equation and the energy dissipation. We like to show that the incompressibility of the fluid follows from the physical property of the fluid at a low Mach number.

The simulation is run until the steady state is reached, a time at which the density and the streamlines of the velocity field are calculated and the results are shown on Fig. 1–Fig. 3.

In the three cases under examination, the density keeps its initial constant value within a 5% tolerance, which defines a small level of compressibility due to the set of equations used. The velocity streamlines are consistent with the expectations in []. The central vortex is moving closer to the center with increasing Reynold number. At  $Re = 400$ , besides the central vortex, two additional vortexes on the lower corners appear. Their size increases with higher Reynold number. In addition the appearance of a vortex on the top left corner for the higher Reynold number  $Re = 3200$  guarantees the correctness of the kinetic consistent equations used in this study.

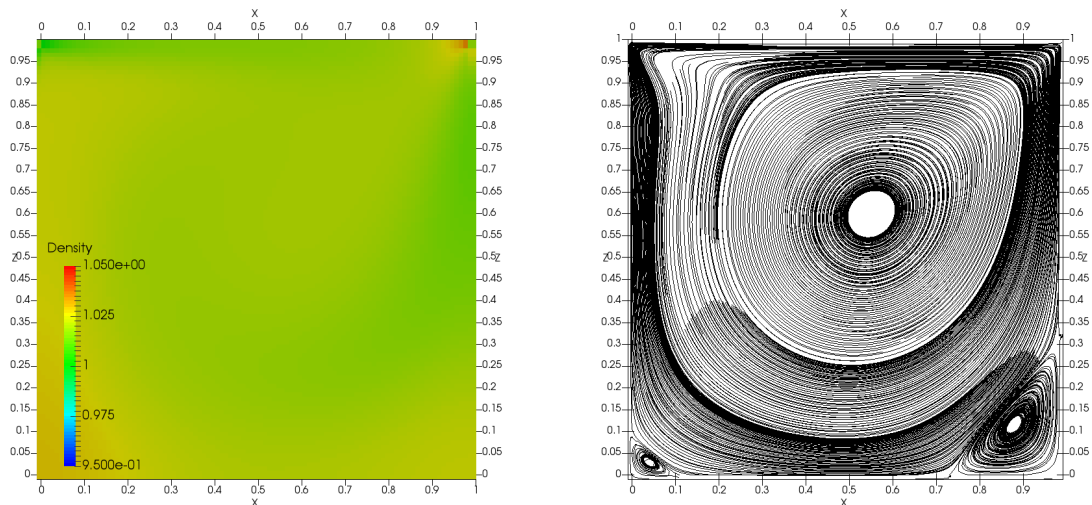


**Figure 1:** Density (left) and streamlines of the velocity field (right) of the lid driven cavity problem with  $Re = 400$ .

### 3.2 Lid driven cavity with liquid sodium

As a second test we repeat the lid-driven cavity test proposed in the previous section using the physical parameters and units for the description of the behavior of liquid sodium. A cavity of size  $0.3 \text{ m} \times 0.3 \text{ m}$  is filled in with liquid sodium. At the initial time the liquid metal is at rest, with initial density  $\rho_0 = 874 \text{ Kg/m}^3$  and temperature  $T = 600^\circ \text{ K}$ . The magnetic field is absent.

The upper lid is moving with a velocity of  $2 \text{ m/s}$ , which defines a Mach number of  $0.005$ . This is a typical value of the stream velocity of liquid metal systems.

The liquid sodium viscosity and thermal conductivity are calculated with the empirical formulation from tabulated data [6]:

$$\mu = \exp \left( -6.4406 - 0.3958 \log T + \frac{556.835}{T} \right) \quad (15)$$

$$k = -124.67 - 0.11381T + 5.5226 \times 10^{-5}T^2 - 1.1842 \times 10^{-8}T^3 \quad (16)$$

The value of  $\tau$  in the kinetic algorithm is calculated as in Eq. 14.

The computational domain is decomposed into  $128 \times 128$  cells, the mesh size being then  $h = 2.34375 \text{ mm}$ . As above the boundary conditions are open for all variables, except for the velocity, which is set to 0 on the  $x = 0, x = 1, z = 0$  borders and to  $2 \text{ m/s}$  on the  $z = 1$  border.

Although also this test does not include the magnetic field, it is a necessary step for the evaluation of the modeling performance. We aim at showing that, using a more realistic set of parameters for the description of the liquid sodium, the structure of the streamlines of the velocity field assumes specific features, which can not be easily included

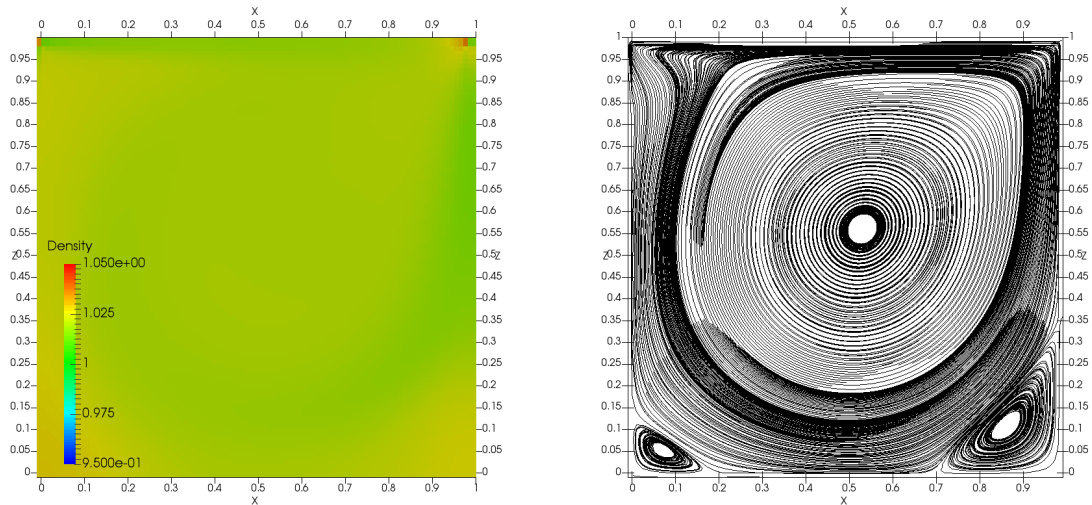


**Figure 2:** Density (left) and streamlines of the velocity field (right) of the lid driven cavity problem with  $Re = 1000$ .

in the previous lid-driven cavity normalized problem. Moreover as before the set of kinetic consistent equations used in this study includes the density continuity equation and the energy dissipation. We like to show that the non compressibility of the liquid sodium follows from the physical property of the fluid at a low Mach number.

In Fig. 4 we show the solution at time  $t = 1s$ . Although it is far from the steady state, the vortex structure inset is clearly visible. We plan to extend the simulation to further time, in order to study the vortex structure at the steady state. The density is constant, with the exception of the points at the edges of the lid, which are well-known as discontinuity points in this test. Thus also the compressible-fluid approximation of the solution is preserved at initial times by the kinetic consistent set of equations used in the calculation.

### 3.3 Liquid sodium flow in pipe with magnetohydrodynamic pump

In this third numerical test we include the magnetic field for the simulation of a prototype of a liquid sodium magnetic pump pipe. This problem arises in the cooling systems of high-density thermal power, which require fluids with high thermal conductivity, such as liquid metals. Electromagnetic pumps are used in liquid metal flow control in cooling systems. The operation of the electromagnetic pump used for the flow control is based on the Faraday principle, where the electric current and the magnetic field interaction generates the magnetic driving force which produces the metallic fluid flow [7]. This type of equipment can control a high conductivity liquid metal flow in a close circuit and facilitates natural circulation in the event of failures or accidents, which is highly convenient for the safety of nuclear reactors.

In this simulation a 2-dimensional pipe with dimensions  $0.3\text{ m} \times 0.1\text{ m}$  is filled with liquid

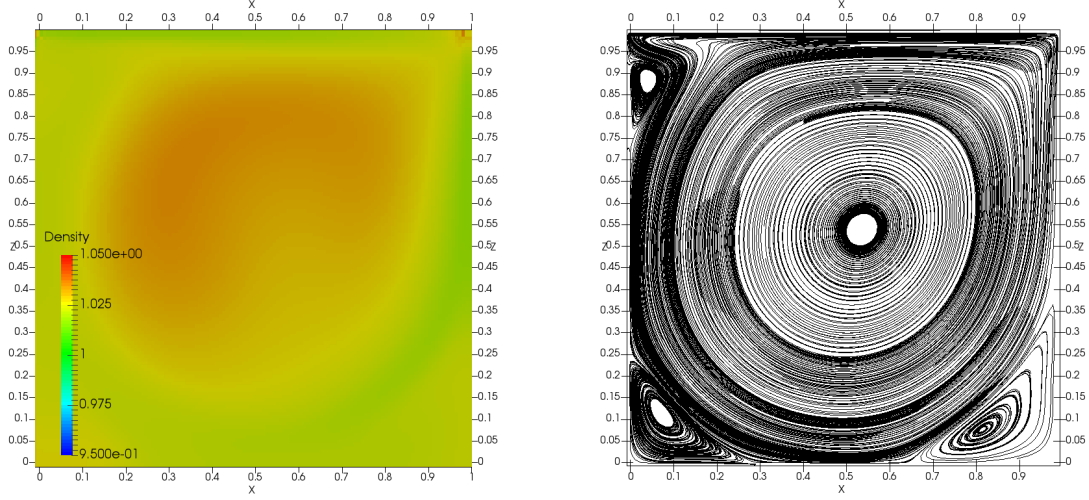


**Figure 3:** Density (left) and streamlines of the velocity field (right) of the lid driven cavity problem with  $Re = 3400$ .

sodium. At the initial time the liquid metal is at rest, with initial density  $\rho_0 = 878 \text{ Kg/m}^3$  and temperature  $T = 600^\circ \text{ K}$ . In the first portion of the pipe, at  $x < 0.1 \text{ m}$ , an external current is placed, with direction perpendicular to the pipe and strength  $I = 800 \text{ A}$ . In the same portion of the pipe and initial magnetic field directed along the y-axis is placed, with strength  $B = 0.05 \text{ T}$ . These magnetic field and current provide the driving force of the liquid meal flow.

Border conditions are open for all variables at all boundaries, with the exception of the velocity, which is set to 0 at the upper and lower boundaries. The liquid sodium viscosity and thermal conductivity are calculated with the empirical formulation from tabulated data [6] as in Eq. 15 and Eq. 16. The resistivity is calculated also from tabulated data:

$$\mu_b = \left( -9.9141 + 8.2022 \times 10^{-2}T - 1.3215 \times 10^{-4}T^2 + 1.7272 \times 10^{-7}T^3 - 9.0265 \times 10^{-11}T^4 + 1.9553 \times 10^{-14}T^5 \right) \times 10^{-8} \quad (17)$$

The results of the numerical modeling are shown on Fig. 5 at a time  $t = 10 \text{ ms}$ . Following the magnetic force induced by the magnetic field and he current, a flow is organized in the pipe. The profile of the velocity flow is shown on Fig. 6 and is in agreement with a laminar flow hypothesis. The velocity flow has a maximum strength of  $2.5 \text{ m/s}$  in the center of the pipe. The density is uniform within a tolerance of 3%, which provides also the magnitude of the compressible liquid approximation in the kinetic consistent equations used in this study. The magnetic field lines are distorted and smoothed, as as result of the interaction with the produced flow and of the liquid sodium resistivity.

This test is the first successful step for the demonstration of the use of the kinetic consistent magneto gas dynamics equations in the modeling of the magnetic pump flow for liquid metals.

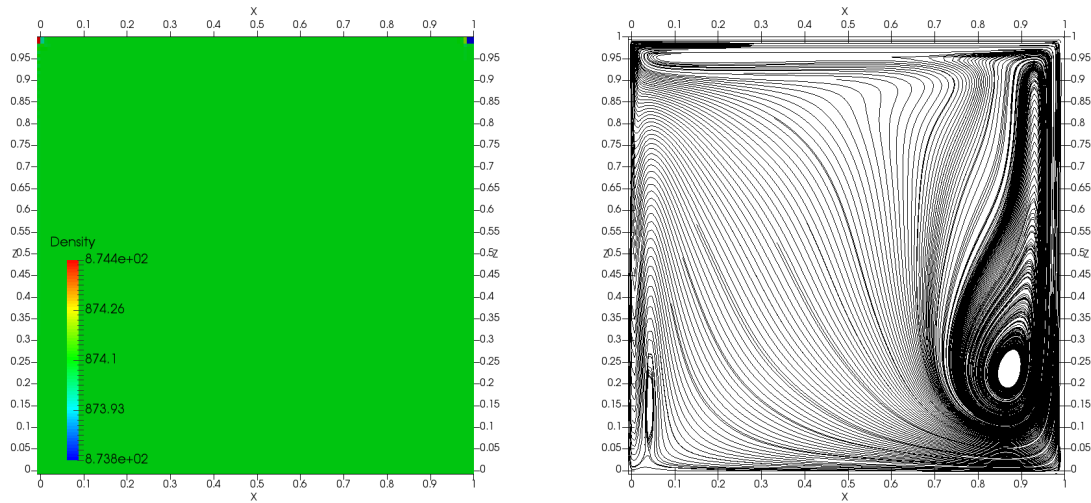


**Figure 4:** Density (left) and streamlines of the velocity field (right) of the lid driven cavity problem for liquid sodium at time  $t=1s$  .

## 4 CONCLUSIONS

Kinetic consistent model previously is used for the mathematical modeling of the ionized gases, can be successfully used for the mathematical modelling of the incompressible conducting liquid flow (magnetohydrodynamic problems). Proposed algorithm is important for mathematical modelling of the processes in number of the important technological systems at parallel high performance computing systems.

## ACKNOWLEDGEMENT

This study was supported by Russian Science Foundation grant 14-11-00170

## REFERENCES

- [1] B.N. Chetverushkin, N. DAscenzo, V.I. Saveliev, Kinetically Consistent Magneto-gasdynamic Equations and Their Use in Supercomputer Computations, *Dokl. Math, RAS.* (2014) **90**:495-498.
- [2] B.N. Chetverushkin, N. DAscenzo, V.I. Saveliev, Kinetically Consistent Magneto-gasdynamic Equations and Their Use in Supercomputer Computations, *Dokl. Math, RAS.* (2014) **90**:495-498.
- [3] B.N. Chetverushkin, N. DAscenzo, V.I. Saveliev, Hyperbolic type explicit kinetic scheme of magneto gas dynamics for high performance computing systems, *Russ. J. Num. Anal. Math. Model.* (2015) **30** 27-36.



- [4] Chia U., Chia K.N., Shin C.T. High Re Solutions for Incompressible Flow Using the Navier-Stokes Equations and a Multigrid Method. *J. of Computational Physics* (1982) **48**:384–411.
- [5] J.L.Sohn Evaluation of Fidap on some Classical Laminar and Turbulent Benchmarks *Int. J. for Num. Meth. in Fluids* (1998) **8**:1469–1490.
- [6] J.K. Fink and L. Leibowitz, *Thermodynamic and transport properties of sodium liquid and vapor*, ANL/RE-95/2, 1995.
- [7] E. M. Borges, F.A. Braz Filbo, L. N. F. Guimaraes, *Liquid metal flow control by DC electromagnetic pump*, Thermal Engineering, (2010) **9** 47-54.
- [8] U.Chia, K.N.Chia and C.T.Shin, *Thermodynamic and transport properties of sodium liquid and vapor*, ANL/RE-95/2, 1995.
- [9] J.K. Fink and L. Leibowitz, *Thermodynamic and transport properties of sodium liquid and vapor*, ANL/RE-95/2, 1995.

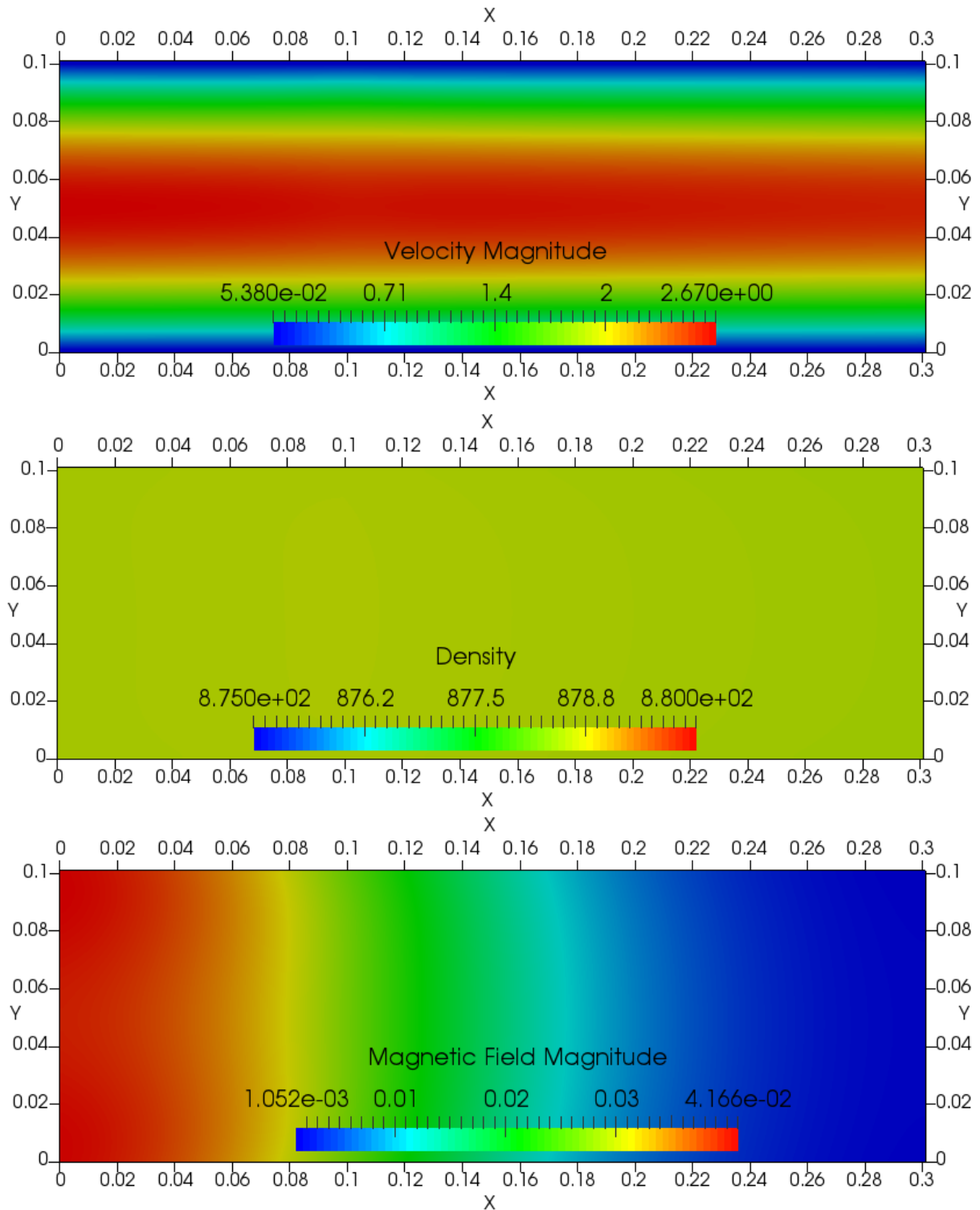


**Figure 5:** Density, magnetic field and velocity of the liquid sodium magnetic pump pipe problem at  $t=10$  ms.

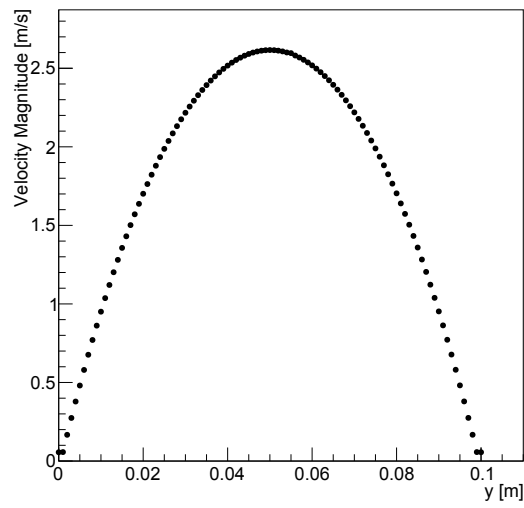


**Figure 6:** Profile of the velocity magnitude along a line parallel to the y-axis for the liquid sodium magnetic pump pipe problem at  $t=10$  ms.